

**Supplementary Information for**

**Toward Rational Design of Organic Electron Acceptor for**

**Photovoltaics: a Study Based on Perylenediimide Derivatives**

Qifan Yan, Yan Zhou, Yu-Qing Zheng, Jian Pei\* and Dahui Zhao\*

jianpei@pku.edu.cn, dhzhao@pku.edu.cn

**Table of contents**

<b>I. Syntheses and characterizations.....</b>	<b>S2</b>
<b>II. UV-vis absorption and cyclic voltammetry measurements.....</b>	<b>S6</b>
<b>III. DFT calculations.....</b>	<b>S11</b>
<b>IV. Device fabrication and measurements.....</b>	<b>S13</b>
<b>V. Atomic force microscopy (AFM) and X-ray diffraction study.....</b>	<b>S15</b>
<b>References.....</b>	<b>S16</b>

## I. Syntheses and characterizations

**General Methods.** Chemicals were used as received unless otherwise indicated. All oxygen or moisture sensitive reactions were performed under nitrogen atmosphere using the standard Schlenk method. Reagent grade tetrahydrofuran (THF) was distilled over sodium and benzophenone. Toluene was distilled from sodium. NMR spectra were recorded on a Mercury plus 300 (300 MHz), Bruker-400 (400 MHz), and Bruker-500 (500 MHz) using  $\text{CDCl}_3$  as the solvent unless otherwise noted. Chemical shifts in  $^1\text{H}$  and  $^{13}\text{C}$  NMR spectra were reported in parts per million (ppm) with referencing to TMS (0 ppm) for  $^1\text{H}$  NMR and  $\text{CDCl}_3$  (77.23 ppm) for  $^{13}\text{C}$  NMR, respectively. MALDI-TOF mass spectra were recorded on an ABI 4800 Plus MALDI TOF/TOF Analyzer using CHCA as matrix, or on a Bruker BIFLEX III MALDI TOF spectrometer using CCA as matrix. Elemental analysis was performed on a vario EL elemental analyzer (Elementar Analysensysteme GmbH).

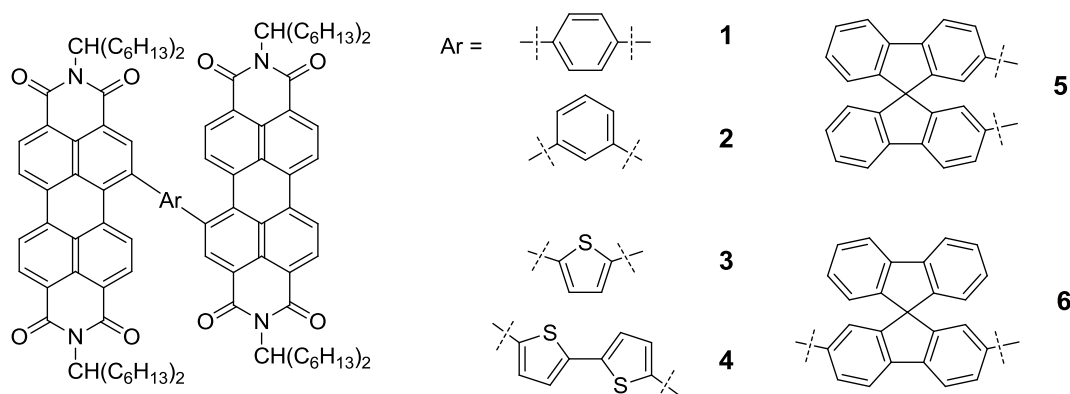
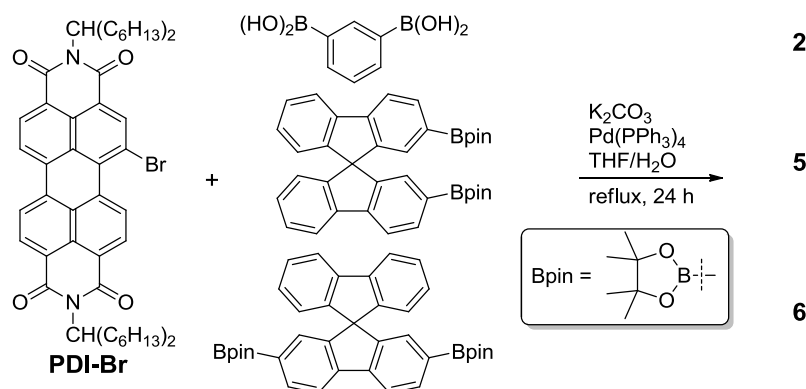


**Chart S1.** Structures of PDI dimers



### General procedure for Suzuki coupling reactions

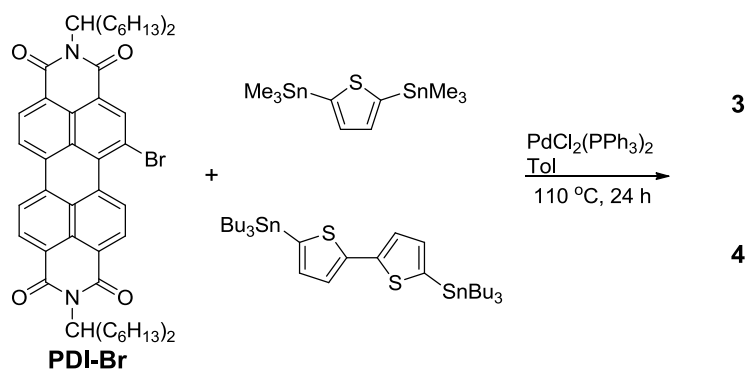
A Schlenk tube charged with **PDI-Br**<sup>S1</sup> (1.0 eq.), corresponding boron acid/ester (0.5 eq.), Pd(PPh<sub>3</sub>)<sub>4</sub> (0.05 eq.), and K<sub>2</sub>CO<sub>3</sub> was evacuated and backfilled with nitrogen for three times, and added with degassed THF (50 mL/1 g **PDI-Br**)/H<sub>2</sub>O (the same as THF). The reaction mixture was heated at reflux for 24 h. After cooled to room temperature, the reaction mixture was diluted with petroleum ether (PE), and then washed with NH<sub>4</sub>Cl (saturated aq.). The organic layer was dried over Na<sub>2</sub>SO<sub>4</sub>, and then concentrated using a rotary evaporator before subjecting to column chromatography over silica gel. The product was eluted with petroleum ether/dichloromethane (PE/DCM) as a red solid after removing solvents.

Compound **2** (66%). <sup>1</sup>H NMR (CDCl<sub>3</sub>, 300 MHz, ppm): δ 7.48-8.71 (m, 18H), 5.13 (m, 4H), 2.21 (m, 8H), 1.82 (m, 8H), 0.90-1.22 (m, 64H), 0.80-0.82 (m, 24H). <sup>13</sup>C NMR (CDCl<sub>3</sub>, 125 MHz, ppm): δ 164.8, 164.4, 163.7, 163.5, 163.4, 163.30, 163.27, 145.6, 145.2, 140.5, 136.6, 136.5, 136.4, 136.1, 135.8, 135.7, 135.2, 134.9, 134.8, 134.6, 134.5, 134.4, 133.0, 132.7, 132.3, 132.0, 131.8, 131.54, 131.48, 131.4, 131.1, 130.74, 130.67, 130.4, 130.1, 130.0, 129.55, 129.47, 129.2, 129.0, 128.9, 128.7, 128.4, 128.2, 127.8, 124.2, 123.9, 123.7, 123.3, 123.1, 122.6, 55.1, 54.9, 32.6, 32.5, 31.9, 29.4, 27.1, 27.0, 22.8, 14.2. MALDI-TOF MS: Calcd for C<sub>106</sub>H<sub>126</sub>N<sub>4</sub>O<sub>8</sub>, 1583.0 (M<sup>+</sup>). Found, 1605.9 (M + Na<sup>+</sup>). Elem. Anal.: Calcd for C<sub>106</sub>H<sub>126</sub>N<sub>4</sub>O<sub>8</sub>, C, 80.37; H, 8.02; N, 3.54. Found, C, 80.32; H, 8.04; N, 3.54.

Compound **5** (78%). <sup>1</sup>H NMR (CDCl<sub>3</sub>, 400 MHz, ppm): 8.47-8.63 (m, 10H), 8.02-8.21 (m, 4H), 7.28-7.83 (m, 7H), 7.15 (t, *J* = 7.4 Hz, 2H), 7.03-7.07 (m, 2H), 6.87-6.90 (m, 2H), 6.75 (s, 1H), 5.15-5.18 (m, 4H), 2.23-2.25 (m, 8H), 1.84 (m, 8H), 1.22-1.27 (m, 64H), 0.83 (m, 24H). <sup>13</sup>C NMR (CDCl<sub>3</sub>, 125 MHz, ppm): δ 165.0, 164.92, 164.86, 164.5, 163.9, 163.8, 163.7, 163.4, 151.7, 151.3, 147.1, 142.9, 142.8, 141.6, 141.5, 139.5, 139.4, 134.9, 134.6, 134.5, 132.9, 132.8, 131.6, 131.5, 130.9, 130.7, 130.2, 130.0, 129.3, 129.2, 129.0, 128.6, 128.4, 128.2, 127.9, 127.6, 124.8, 124.5, 124.0, 123.6, 123.3, 123.1, 122.9, 122.7, 122.3, 121.1, 120.5, 120.2, 66.2, 55.0, 54.8, 32.6, 32.0, 29.4, 27.14, 27.11, 22.84, 22.79, 14.2. MALDI-TOF MS: Calcd for C<sub>125</sub>H<sub>136</sub>N<sub>4</sub>O<sub>8</sub>, 1822.0 (m/z). Found, 1845.4 (M + Na<sup>+</sup>). Elem. Anal.: Calcd for

C<sub>125</sub>H<sub>136</sub>N<sub>4</sub>O<sub>8</sub>, C, 82.38; H, 7.52; N, 3.07. Found, C, 82.19; H, 7.58; N, 3.10.

Compound **6** (80%). <sup>1</sup>H NMR (CDCl<sub>3</sub>, 300 MHz, ppm): δ 8.51-8.63 (m, 10H), 8.00-8.19 (m, 4H), 6.75-7.82 (m, 14H), 5.15-5.17 (m, 4H), 2.23 (m, 8H), 1.83-1.84 (m, 8H), 1.25 (m, 64H), 0.83 (m, 24H). <sup>13</sup>C NMR (CDCl<sub>3</sub>, 125 MHz, ppm): δ 164.9, 164.5, 163.8, 163.4, 151.7, 151.3, 147.1, 142.9, 142.8, 141.54, 141.47, 141.3, 136.5, 135.8, 134.9, 134.5, 132.7, 131.6, 130.9, 130.2, 130.0, 129.2, 129.0, 128.6, 128.4, 128.2, 127.9, 127.6, 124.8, 124.5, 124.0, 123.6, 123.3, 123.1, 122.7, 122.3, 120.4, 120.2, 66.4, 66.2, 55.0, 54.8, 32.6, 32.0, 29.9, 29.4, 27.1, 22.8, 14.2. MALDI-TOF MS: Calcd for C<sub>125</sub>H<sub>136</sub>N<sub>4</sub>O<sub>8</sub>, 1822.0 (m/z). Found, 1821.6 (m/z). Elem. Anal.: Calcd for C<sub>125</sub>H<sub>136</sub>N<sub>4</sub>O<sub>8</sub>, C, 82.38; H, 7.52; N, 3.07. Found, C, 82.25; H, 7.52; N, 3.12.



### General procedure for Stille coupling reactions

A Schlenk tube charged with **PDI-Br** (1.0 eq.), corresponding tin agent (0.5 eq.), and PdCl<sub>2</sub>(PPh<sub>3</sub>)<sub>2</sub> (0.05 eq.) was evacuated and backfilled with nitrogen for three times, and added with degassed toluene (50 mL/1 g **PDI-Br**). The reaction mixture was heat at 110 °C for 24 h. After cooled to room temperature, 2 mL of KF (aq. 1 M) was added to the reaction mixture, and stirred for 2 h. The organic layer was washed with brine, and then dried over Na<sub>2</sub>SO<sub>4</sub>. After concentrated on a rotary evaporator, the residual was subject to column chromatography over silica gel eluted by PE/DCM.

Compound **3** (91%). <sup>1</sup>H NMR (CDCl<sub>3</sub>, 300 MHz, ppm): δ 8.36-8.74 (m, 14H), 7.44 (s, 2H), 5.11-5.21 (m, 4H), 2.16-2.29 (m, 8H), 1.82-1.88 (m, 8H), 1.18-1.31 (m, 64H), 0.76-0.86 (m, 24H). <sup>13</sup>C NMR (CDCl<sub>3</sub>, 125 MHz, ppm): δ 164.8, 164.7, 164.6, 164.5, 163.7, 163.5, 147.0, 136.9, 136.2, 135.0, 134.3, 134.1, 133.8, 132.8, 131.9, 131.8,

131.1, 130.7, 130.0, 129.4, 129.2, 129.0, 128.4, 127.7, 124.2, 124.0, 123.8, 123.6, 123.4, 123.1, 122.7, 55.2, 55.0, 32.64, 32.57, 32.0, 31.9, 29.5, 29.4, 27.2, 27.1, 22.82, 22.77, 14.3, 14.1. MALDI-TOF MS: Calcd for  $C_{104}H_{124}N_4O_8S$ , 1588.9 ( $M^+$ ). Found, 1611.2 ( $M + Na^+$ ). Elem. Anal.: Calcd for  $C_{104}H_{124}N_4O_8S$ , C, 78.55; H, 7.86; N, 3.52. Found, C, 78.50; H, 7.97; N, 3.49.

Compound **4** (74%).  $^1H$  NMR ( $CDCl_3$ , 300 MHz, ppm):  $\delta$  8.43-8.70 (m, 14H), 7.24-7.29 (m, 4H), 5.18-5.20 (m, 4H), 2.24-2.26 (m, 8H), 1.85 (m, 8H), 1.22-1.29 (m, 64H), 0.79-0.83 (m, 24H).  $^{13}C$  NMR ( $CDCl_3$ , 125 MHz, ppm):  $\delta$  164.9, 164.6, 163.9, 163.8, 163.7, 163.6, 163.5, 143.8, 139.4, 137.1, 136.5, 135.1, 134.4, 134.3, 133.8, 133.2, 131.8, 131.13, 131.1, 130.4, 129.9, 129.4, 129.1, 128.31, 128.27, 127.7, 126.1, 124.3, 123.9, 123.6, 123.4, 123.1, 122.9, 122.5, 55.1, 55.0, 32.6, 31.98, 31.96, 29.4, 27.1, 22.80, 22.78, 14.24, 14.23. MALDI-TOF MS: Calcd for  $C_{108}H_{126}N_4O_8S_2$ , 1670.9 ( $M^+$ ). Found, 1693.9 ( $M + Na^+$ ). Elem. Anal.: Calcd for  $C_{108}H_{126}N_4O_8S_2$ , C, 77.57; H, 7.59; N, 3.35. Found, C, 77.38; H, 7.69; N, 3.37.

## II. UV-vis absorption and cyclic voltammetry measurements

UV-vis absorption spectra were recorded on a Hitachi U-4100 spectrophotometer or a Perkin-Elmer Lambda 750 UV-vis spectrometer using the absorption mode in a 1-cm quartz cell for solution sample. The temperature of the sample was controlled using a circulated liquid (water + glycol) bath with a DC-2006 temperature control unit (Ningbo SCIENTZ Biotechnology Co., Ltd, China).

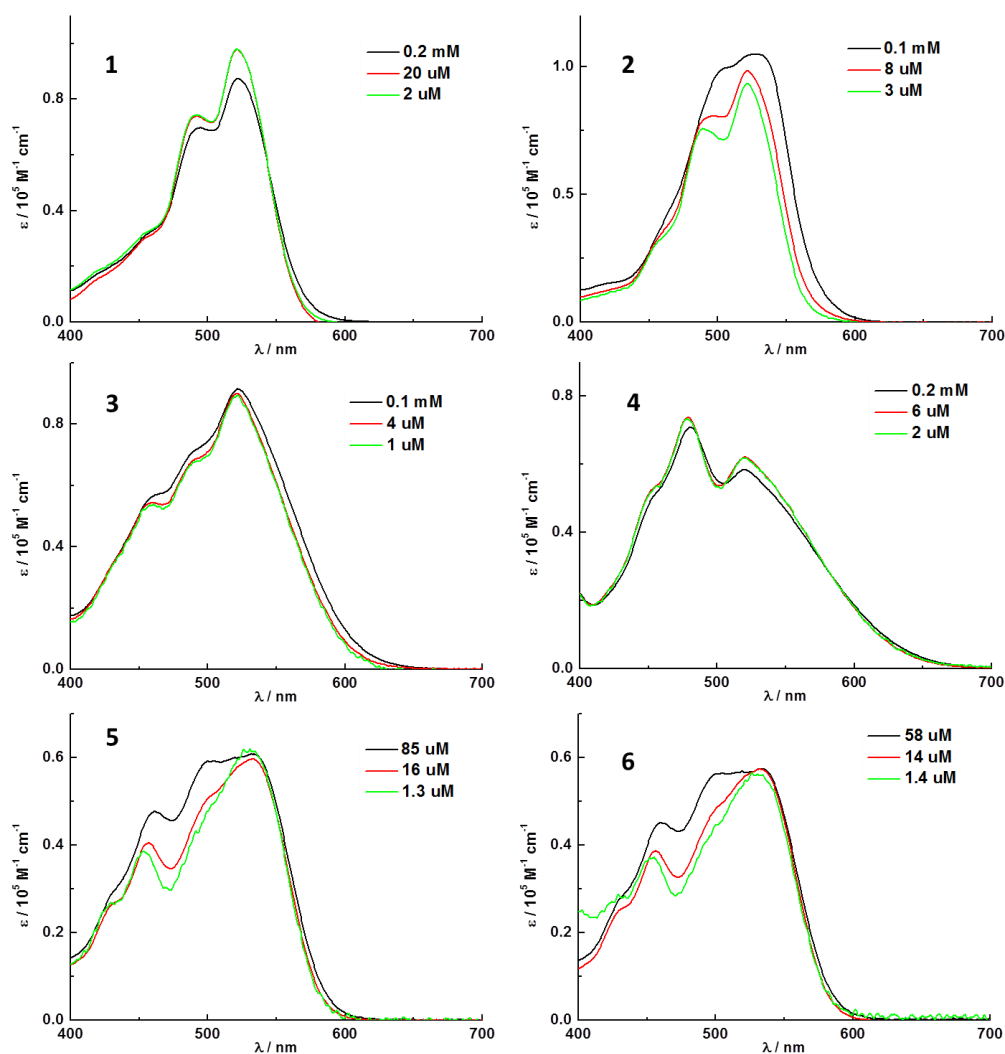


**Figure S1.** UV-vis absorption spectra of **1-6** in cyclohexane solution at different concentrations (spectra recorded at room temperature).

The absorption spectra of **1**, **3**, and **4** remained almost unchanged at varied concentrations, suggesting minimal intermolecular interactions of these molecules in

solution (Fig. S1). For **5** and **6**, certain band shape change was observed at higher concentrations, but the alterations mainly occurred in the short-wavelength region. The main absorption peak (originating from PDI units) and onset remained unchanged, which indicate that certain intermolecular interactions emerged at higher concentrations, but they more likely are related to the spirobifluorene linker instead of PDI groups. In contrast, as the solution concentration increased, the absorption spectrum of **2** displayed evident band shape change in the wavelength range that's attributable to the PDI units, which evidenced the intermolecular interactions of **2** involving the aggregation of PDI moieties. Therefore, a temperature dependency study was then performed for **2** in order to obtain the association constant as well as enthalpy and entropy changes of the aggregation process.

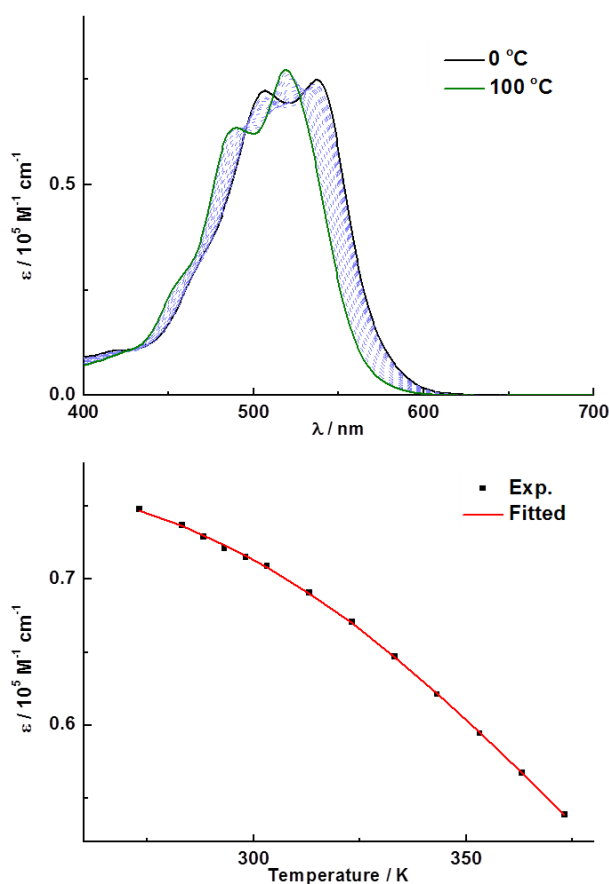


**Figure S2.** Temperature-dependent UV-vis absorption spectra of **2** in dodecane (0.2 mM) and fitting of the absorbance data to Eq. S1 (fitted thermodynamic parameters for dimerization of **2**:  $\Delta H = -39.2 \text{ kJ mol}^{-1}$ ,  $\Delta S = -31.6 \text{ J K}^{-1} \text{ mol}^{-1}$ ,  $K_{298\text{K}} = 1.7 \times 10^5 \text{ M}^{-1}$ )

The apparent extinction coefficients of **2** at 537 nm as a function of temperature were fitted by nonlinear regression analysis to the following expressions.<sup>S2</sup>

$$\varepsilon = ((8Kc + 1)^{0.5} - 1)/4/K/c \times \varepsilon_m + (1 - ((8Kc + 1)^{0.5} - 1)/4/K/c) \times \varepsilon_a \quad (\text{S1})$$

where  $\varepsilon$  is the apparent extinction coefficient;  $\varepsilon_m$  and  $\varepsilon_a$  are the extinction coefficient of the monomer and aggregated species, respectively and  $c$  is the total concentration of the compounds.  $K$  is the dimerization constant. Here, a monomer-dimer equilibration is employed, since based on the calculations (vide infra) **2** in the low-energy conformations should tend to undergo dimerization.  $K$  is also related to the van't Hoff equation (S2):

$$K = \exp((T\Delta S - \Delta H)/RT) \quad (\text{S2})$$

where  $T$  is the absolute temperature,  $\Delta S$  is the entropy change,  $\Delta H$  is the enthalpy change, and  $R$  is the ideal gas constant of  $8.314 \text{ J K}^{-1} \text{ mol}^{-1}$ . Using this dimerization model, the fitted thermodynamic constants are as follows:  $\Delta H = -39.2 \text{ kJ mol}^{-1}$ ,  $\Delta S = -31.6 \text{ J K}^{-1} \text{ mol}^{-1}$ , and  $K_{298\text{K}} = 1.7 \times 10^5 \text{ M}^{-1}$

Absorptions of **1-6** in thin films were then investigated. The films were prepared under the exact same conditions for solar cell device fabrications (vide infra), except that P3HT was replaced by polystyrene (PS). This is because P3HT absorbs strongly in the same wavelength range where **1-6** absorb (Fig. S11). In order to remove the absorption interference of P3HT while still mimicking the condensed state of the acceptors in solar cells, we used PS to replace P3HT. Solutions of **1-6** (mixed with PS at 1:1 weight ratio) in *o*-dichlorobenzene at  $20 \text{ mg mL}^{-1}$  were spin-casted onto ZnO treated substrates. UV-vis spectra of the resultant thin films were recorded (Fig. S3-S5). The hump detected between at 650-700 nm in these spectra is found to result from certain interactions of **1-6** with ZnO treated substrate. Such hump was not observed if we cast the films onto quartz slides. Nor was it observed with blank ITO/ZnO. The absorption spectra of **1-6** in thin films mostly resemble those recorded at higher concentrations in aliphatic solutions.

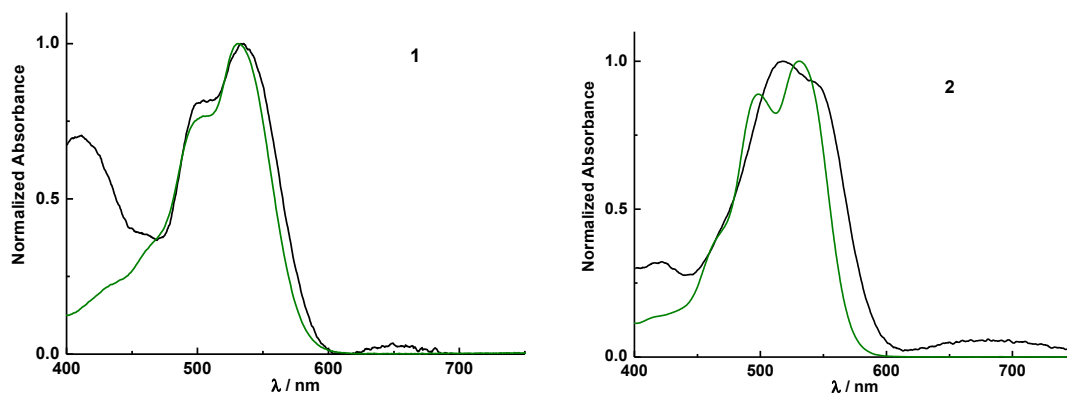


**Figure S3.** UV-vis absorption spectra of **1** and **2** in  $\text{CH}_2\text{Cl}_2$  solutions (green line, 10  $\mu\text{M}$ ) and in thin films (black line, mixed with polystyrene) at room temperature.

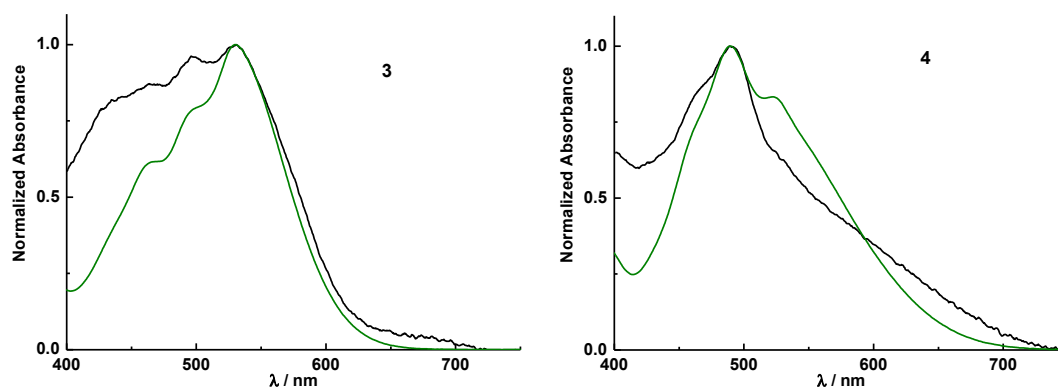


**Figure S4.** UV-vis absorption spectra of **3** and **4** in  $\text{CH}_2\text{Cl}_2$  solutions (green line, 10  $\mu\text{M}$ ) and in thin films (black line, mixed with polystyrene) at room temperature.

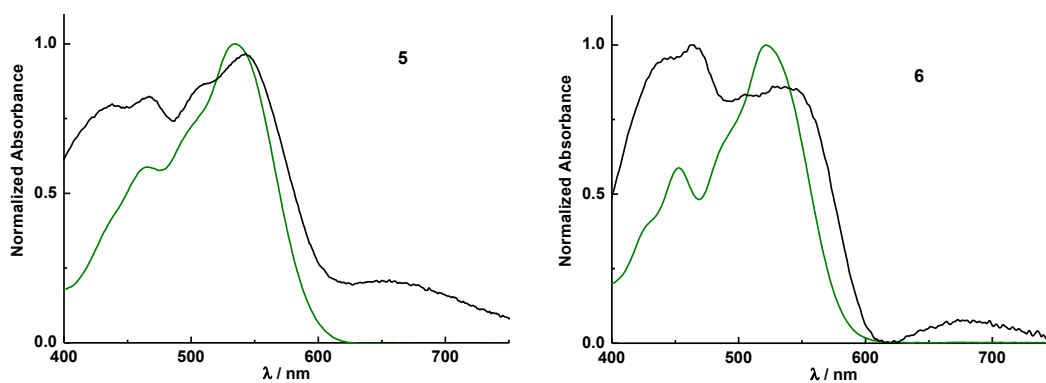


**Figure S5.** UV-vis absorption spectra of **5** and **6** in  $\text{CH}_2\text{Cl}_2$  solutions (green line, 10  $\mu\text{M}$ ) and in thin films (black line, mixed with polystyrene) at room temperature.

Cyclic voltammetry was carried out on a BASI Epsilon electrochemical workstation with three electrodes configuration, using Ag/AgCl as the reference electrode, a Pt plate as the counter electrode, and a glassy carbon as the working electrode. Samples were dissolved in methylene chloride with 0.1 M Bu<sub>4</sub>NPF<sub>6</sub> as the supporting electrolyte for cyclic voltammetry measurements. The scan speed is 100 mV s<sup>-1</sup>. The solution concentrations are all 0.1 mM. The solutions were degassed by bubbling nitrogen for one minute before electrochemical measurements.

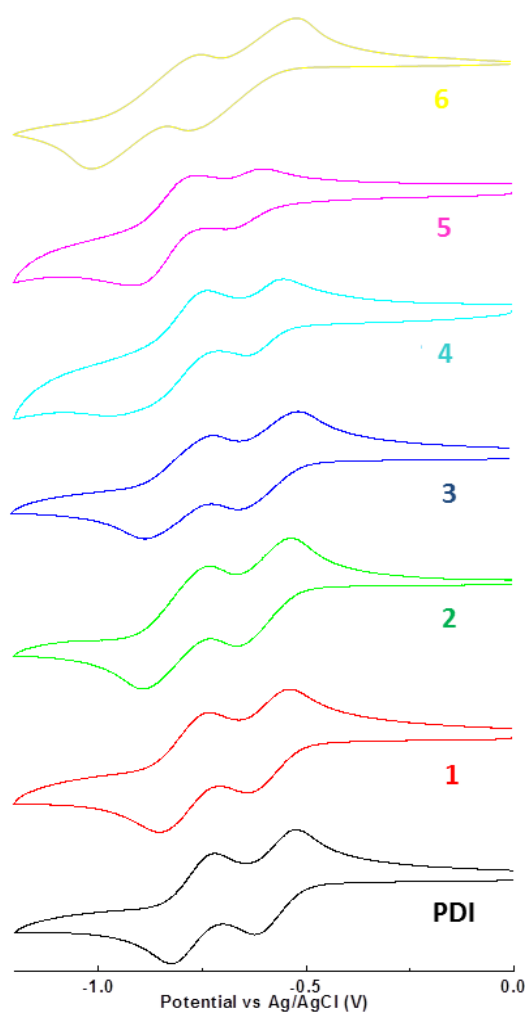


**Figure S6.** Reductive cyclic voltammograms of **1-6** in comparison with **PDI**.

### III. DFT calculations

The geometry was optimized with Density Functional Theory (DFT) using B3LYP hybrid functional<sup>S3</sup> with a basis set limited to 6-31g\*\*. TD-DFT calculations were performed at optimized geometries using the same theory level. Quantum-chemical calculation was performed with the Gaussian03<sup>S4</sup> package and the orbital pictures were prepared using Gaussview.<sup>S5</sup> All *N*-hexylheptyl substituents were replaced with methyl groups in calculations.

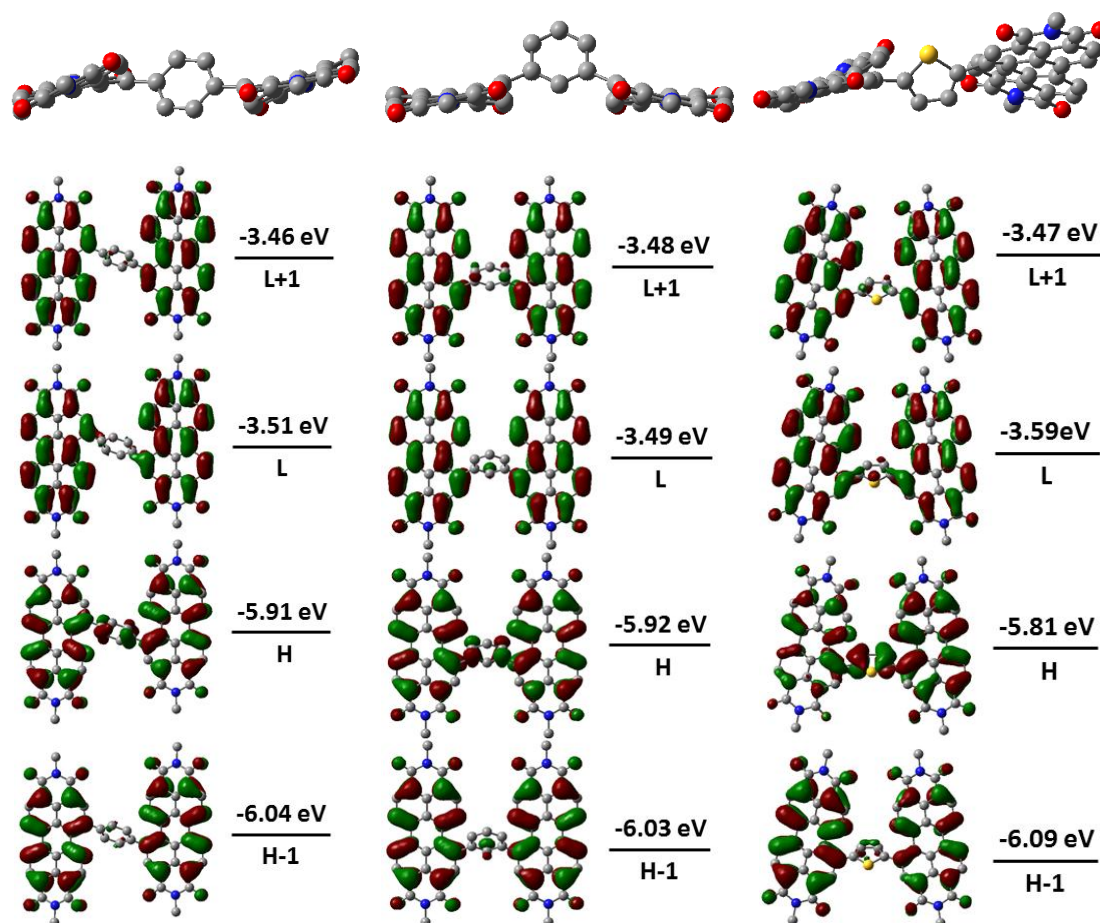


**Figure S7.** DFT calculated geometry (hydrogen atoms omitted) and FMOs of **1-3**. (from left to right)

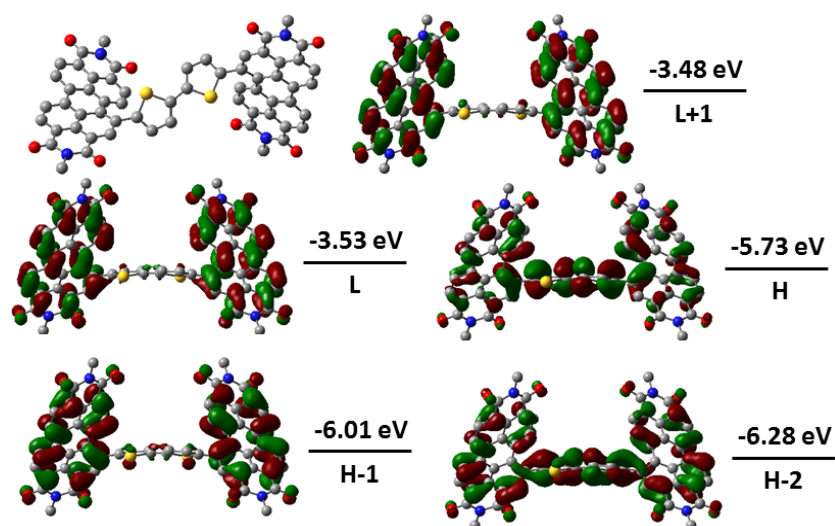


**Figure S8.** DFT calculated geometry (hydrogen atoms omitted) and FMOs of 4.

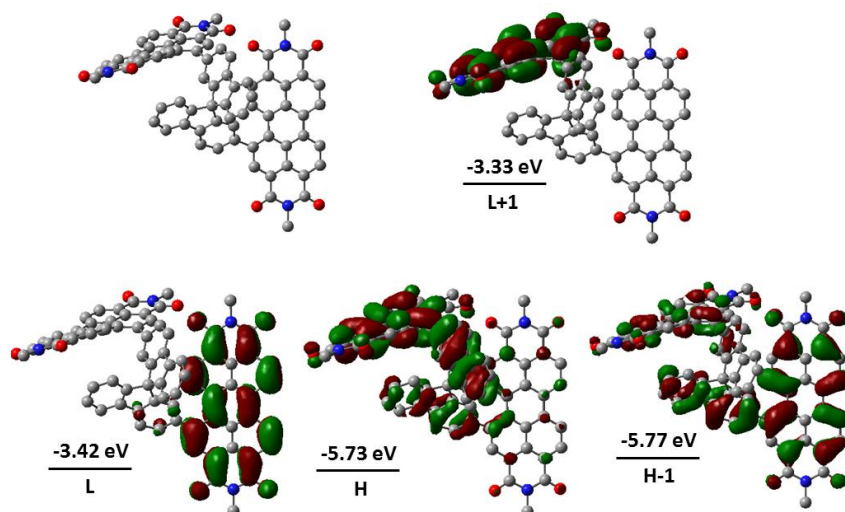


**Figure S9.** DFT calculated geometry (hydrogen atoms omitted) and FMOs of 5.

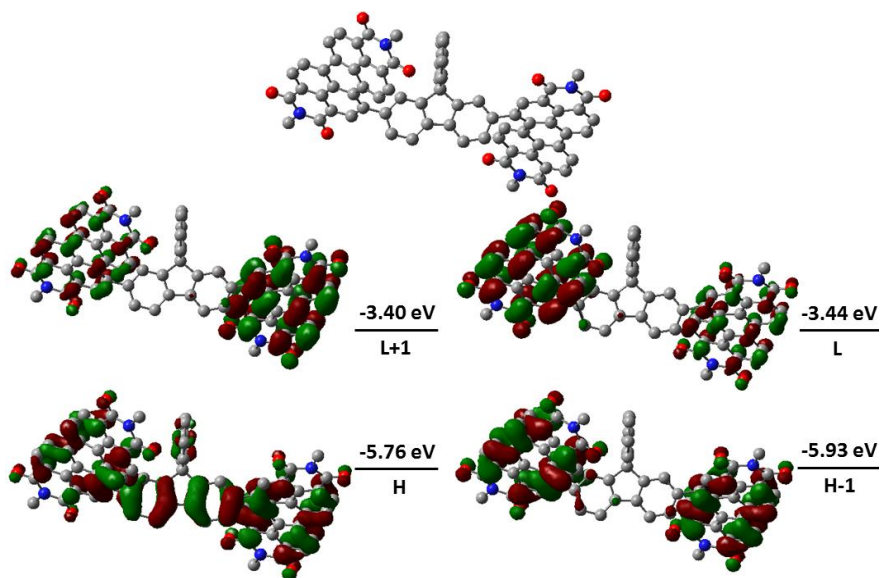


**Figure S10.** DFT calculated geometry (hydrogen atoms omitted) and FMOs of 6.

## IV. Device fabrication and measurements

### Preparation of the ZnO Precursor:

Zinc acetate dihydrate ( $\text{Zn}(\text{CH}_3\text{COO})_2 \cdot 2\text{H}_2\text{O}$ , 1.0 g) and ethanolamine ( $\text{NH}_2\text{CH}_2\text{CH}_2\text{OH}$ , 0.28 g) were dissolved in 2-methoxyethanol ( $\text{CH}_3\text{OCH}_2\text{CH}_2\text{OH}$ , 10 mL) under stirring for 12 h.

### Fabrication of inverted solar cells:

Before dried in a vacuum oven at 80 °C and 15 minutes of oxygen plasma treatment, ITO-coated glass substrates were cleaned with acetone, detergent, distilled water and isopropanol in an ultrasonic bath. After all the preparation, ZnO precursor was spin-coated on the glass at the speed of 4000 rpm for 30 s. The substrates were then annealed at 150 °C in air and transferred into nitrogen-filled glove box for spin-casting the P3HT:PDI-acceptors (at 1:1 weight ratio) in *o*-dichlorobenzene at a concentration of 20 mg mL<sup>-1</sup>. All the blend films were dried at room temperature overnight. Subsequently, 15 nm layer of MoO<sub>3</sub> and 65 nm Ag were thermally deposited sequentially on the active layer covered by a shadow mask under the pressure of  $3.5 \times 10^{-4}$  Pa. The area of devices was 15 mm<sup>2</sup>.

### Measurements of solar cells:

The thickness of the active layer was measured by a surface profiler. P3HT:**1-4** layers were measured to be 120 nm, and P3HT:**5-6** layers were measured to be 180 nm. Solar cell performance were tested under an Air Mass 1.5 Global (AM 1.5G) with irradiation intensity of 100 mW/cm<sup>2</sup> (Newport Solar Simulator 94021A) calibrated by a NREL certified standard silicon cell (4 cm<sup>2</sup>). J-V curves were measured using a Keithley 2636A semiconductor analyzer. An IPCE measuring system with monochromic illumination (Newport 74125 monochromator equipped with a 66984 ARC lamp) was used to carry out IPCE test. The calibration of the incident light intensity was tested with a calibrated silicon photodiode.

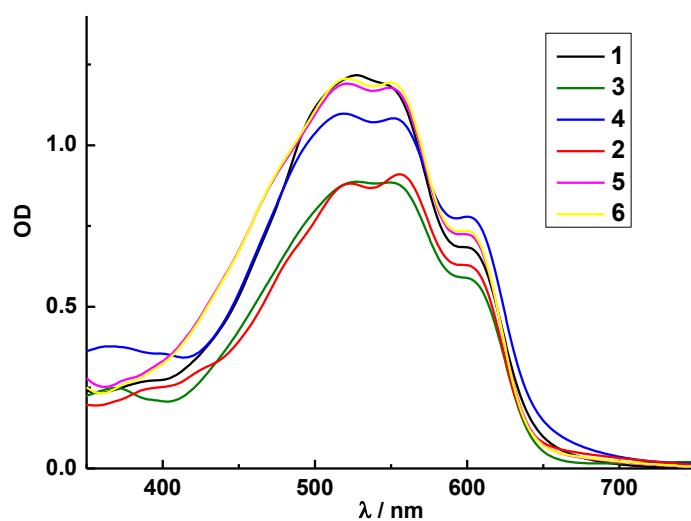


**Figure S11.** UV-vis absorption spectra of active layers P3HT:**1-6** on ITO/ZnO substrate

SCLC electron mobility of compounds **1-6** was calculated by fitting the J-V curve to the following equation:

$$J = 9/8 * \epsilon_0 * \epsilon_r * V^2 / L^3 * \mu$$

where J is the current density,  $\epsilon_0$  is the permittivity of vacuum,  $\epsilon_r$  is the relative permittivity of the material (assumed to be 3.5), V is the voltage, L is the thickness of the film (120 nm for **1-4**, 180 nm for **5-6**),  $\mu$  is mobility of electrons.

## V. Atomic force microscopy (AFM) and X-ray diffraction study

AFM was carried out on a Nanoscope IIIa (Veeco Inc.) atomic force microscopy. Solar cell active layers on ITO/ZnO substrates prior to thermal deposition of metal electrode were subjected to AFM studies. X-ray diffraction pattern of ITO/ZnO/P3HT:PDI-acceptors was recorded on a Rigaku D/max-rA12KW X-ray system.

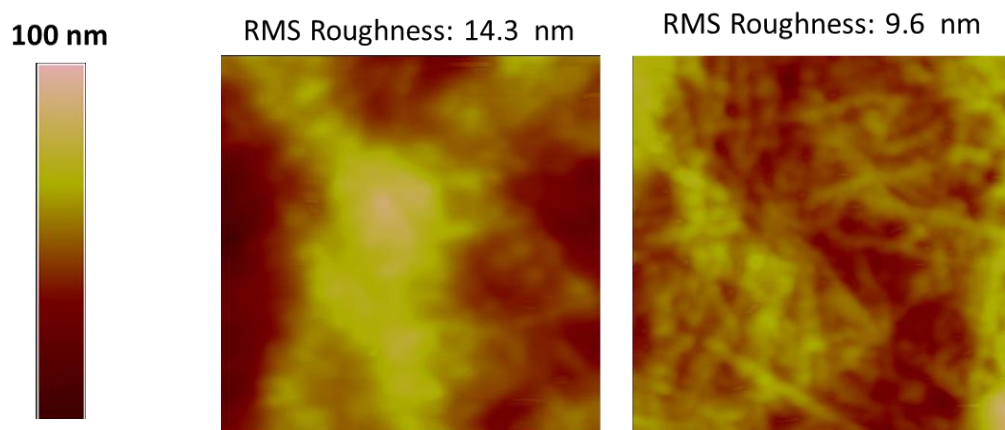


**Figure S12.** AFM images of active layers P3HT:1 (left) and P3HT:2 (right) on ITO/ZnO substrates. The dimension of the images were  $10\ \mu\text{m} \times 10\ \mu\text{m}$ .

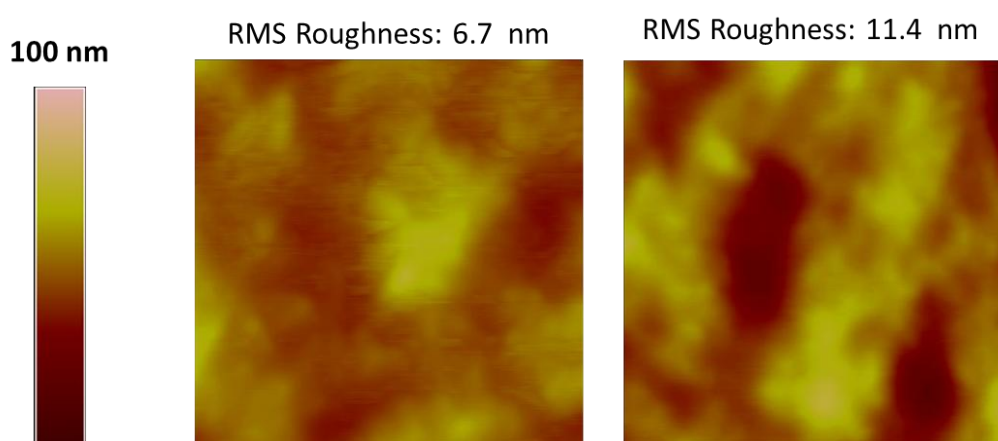


**Figure S13.** AFM images of active layers P3HT:3 (left) and P3HT:4 (right) on ITO/ZnO substrates. The dimension of the images were  $10\ \mu\text{m} \times 10\ \mu\text{m}$ .

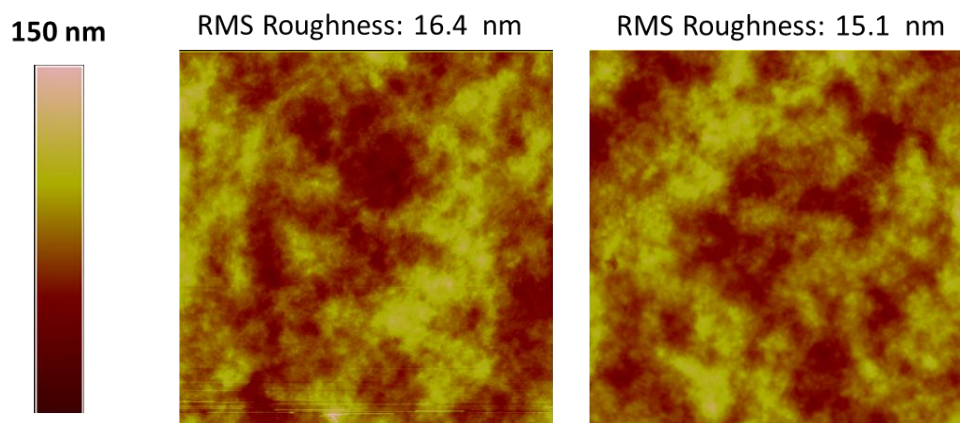


**Figure S14.** AFM images of active layers P3HT:5 (left) and P3HT:6 (right) on ITO/ZnO substrates. The dimension of the images were  $10\ \mu\text{m} \times 10\ \mu\text{m}$ .

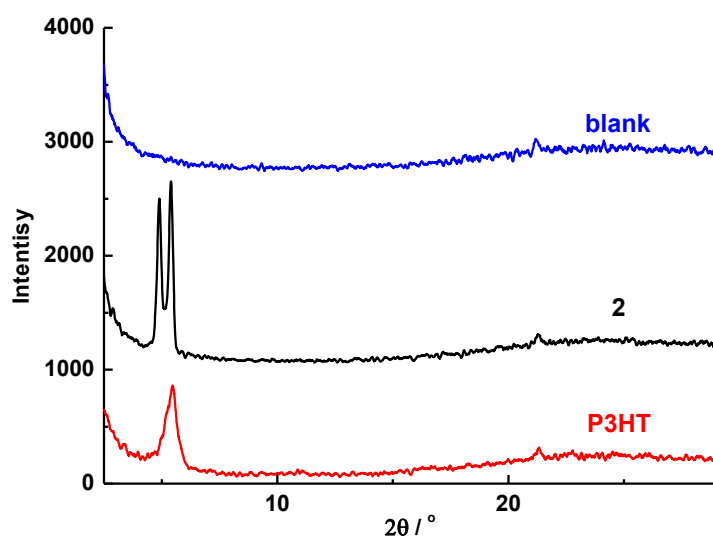


**Figure S15.** X-ray diffraction patterns of pure P3HT and **2** on ITO/ZnO substrate, in comparison with that of blank ITO/ZnO substrate.

## References

- S1. Q. Yan and D. Zhao, *Org. Lett.*, 2009, **11**, 3426.
- S2. Z. Chen, A. Lohr, C. R. Saha-Möller and F. Würthner, *Chem. Soc. Rev.* 2009, **38**, 564-584.
- S3. (a) A. D. Becke, *Phys. Rev. A*, 1988, **38**, 3098–3100. (b) C. Lee, W. Yang, G. G. Parr, *Phys. Rev. B*. 1988, **37**, 785–789.

S4. M. J. Frisch, G. W. Trucks, H. B. Schlegel, G. E. Scuseria, M. A. Robb, J. R. Cheeseman, J. A. Jr. Montgomery, T. Vreven, K. N. Kudin, J. C. Burant, J. M. Millam, S. S. Iyengar, J. Tomasi, V. Barone, B. Mennucci, M. Cossi, G. Scalmani, N. Rega, G. A. Petersson, H. Nakatsuji, M. Hada, M. Ehara, K. Toyota, R. Fukuda, J. Hasegawa, M. Ishida, T. Nakajima, Y. Honda, O. Kitao, H. Nakai, M. Klene, X. Li, J. E. Knox, H. P. Hratchian, J. B. Cross, C. Adamo, J. Jaramillo, R. Gomperts, R. E. Stratmann, O. Yazyev, A. J. Austin, R. Cammi, C. Pomelli, J. W. Ochterski, P. Y. Ayala, K. Morokuma, G. A. Voth, P. Salvador, J. J. Dannenberg, V. G. Zakrzewski, S. Dapprich, A. D. Daniels, M. C. Strain, O. Farkas, D. K. Malick A. D., Rabuck, K. Raghavachari, J. B. Foresman, J. V. Ortiz, Q. Cui, A. G. Baboul, S. Clifford, J. Cioslowski, B. B. Stefanov, G. Liu, A. Liashenko, P. Piskorz, I. Komaromi, R. L. Martin, D. J. Fox, T. Keith, M. A. Al-Laham, C. Y. Peng, A. Nanayakkara, M. Challacombe, P. M. W. Gill, B. Johnson, W. Chen, M. W. Wong, C. Gonzalez, J. A. Pople, *Gaussian 03*, Revision C.02; Gaussian Inc.: Wallingford CT, 2004.

S4. R. H. Dennington, T. Keith, J. Millam, K. Eppinnett, W. L. Hovell, R. Gilliland, *GaussView*, Version 3.09; Semichem, Inc.: Shawnee Mission, KS, 2003.